Front. Environ. Sci. Eng. 2023, 17(3): 27
https://doi.org/10.1007/s11783-023-1627-y

RESEARCH ARTICLE

Removal of virus aerosols by the combination of filtration and UV-C irradiation

Min Shang[1,2], Yadong Kong[1], Zhijuan Yang[3], Rong Cheng (✉)[1], Xiang Zheng (✉)[1], Yi Liu[2], Tongping Chen[2]

1 School of Environment and Natural Resources, Renmin University of China, Beijing 100872, China
2 Sichuan Solid Waste and Chemicals Management Center, Chengdu 610031, China
3 Biogas Institute of Ministry of Agriculture and Rural Affairs, Chengdu 610041, China

HIGHLIGHTS

- The removal of virus aerosols by filtration and UV-C irradiation was proposed.
- The filtration efficiency for virus aerosols was affected by the filtration rate.
- The inactivation rate by UV-C was not linear with irradiation intensity or time.
- The virus trapped by filter material had a shielding effect on UV-C irradiation.

ARTICLE INFO

Article history:
Received 2 March 2022
Revised 12 August 2022
Accepted 12 August 2022
Available online 7 September 2022

Keywords:
Filtration system
UV-C irradiation
Virus aerosol
Public health
COVID-19

GRAPHIC ABSTRACT

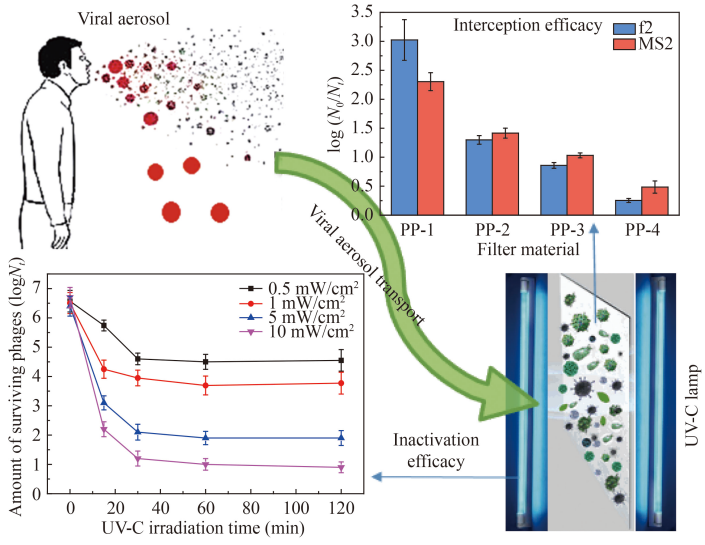

ABSTRACT

The COVID-19 pandemic remains ever prevalent and afflicting—partially because one of its transmission pathways is aerosol. With the widely used central air conditioning systems worldwide, indoor virus aerosols can rapidly migrate, thus resulting in rapid infection transmission. It is therefore important to install microbial aerosol treatment units in the air conditioning systems, and we herein investigated the possibility of combining such filtration with UV irradiation to address virus aerosols. Results showed that the removal efficiency of filtration towards f2 and MS2 phages depended on the type of commercial filter material and the filtration speed, with an optimal velocity of 5 cm/s for virus removal. Additionally, it was found that UV irradiation had a significant effect on inactivating viruses enriched on the surfaces of filter materials; MS2 phages had greater resistance to UV-C irradiation than f2 phages. The optimal inactivation time for UV-C irradiation was 30 min, with higher irradiation times presenting no substantial increase in inactivation rate. Moreover, excessive virus enrichment on the filters decreased the inactivation effect. Timely inactivation is therefore recommended. In general, the combined system involving filtration with UV-C irradiation demonstrated a significant removal effect on virus aerosols. Moreover, the system is simple and economical, making it convenient for widespread implementation in air-conditioning systems.

✉ Corresponding authors
E-mails: chengrong@ruc.edu.cn (R. Cheng);
zhengxiang7825@163.com (X. Zheng)

1 Introduction

COVID-19 is rapidly spreading around the world (Dancer

et al., 2020; Peters et al., 2020; Santos et al., 2020; Bazant and Bush, 2021), and as of December 2021, it has been the cause of the death of more than 5 million people worldwide. Previous studies have confirmed that virus aerosol transmission is one of the most prominent transmission pathways for SARS-CoV-2 as well as for other viral infections (Chen, 2021; Xie et al., 2021). Saliva droplets can carry the virus through the air, or they can evaporate into droplet nuclei and remain airborne for a long time as virus aerosols (Dancer et al., 2020; Peters et al., 2020; Santos et al., 2020; Bazant and Bush, 2021). Although it is difficult for these virus aerosols to spread in enclosed buildings through natural ventilation, the use of central ventilation systems allows virus aerosols to spread over longer distances (Correia et al., 2020; Jiang et al., 2021), thus infecting more people. Considering that people are indoors for 90 % of the day and almost all hyper diffusion events occur indoors (Klepeis et al., 2001; Castrillón and De Lasa, 2007), virus aerosols in enclosed buildings need to be addressed to reduce virus transmissions and infection risk.

Traditional techniques and methods for removing microbial aerosol contamination include increased ventilation, chemical disinfection, air filtration, UV irradiation, photocatalysis and thermal inactivation (Berry et al., 2022). Compared with other techniques, UV irradiation and filtration interception are economical and thus common methods for controlling indoor microbial contamination (Yang et al., 2020; Moreno et al., 2021). Filtration technology can effectively intercept different types of particulate matter, and is thus widely used for removing microbial aerosols from the air (Yang et al., 2020). The main filtration mechanisms are interception, inertial collision and diffusion. The factors affecting filtration efficiency include the size and shape of particles, porosity and thickness of the filter material, and the speed of air flow (Majchrzycka, 2014). Commonly used filter materials for filtering microbial aerosols include glass fiber, polytetrafluoroethylene fiber, polypropylene melt-blown nonwoven fiber, and polycarbonate fiber. According to their different filtration efficiencies, the filter materials are classified into different grades. The efficiency of high-efficiency particulate air (HEPA) filters can reach 99.97 % for particles with sizes of 0.3 μm and above, and they are usually used for microbial aerosol filtration in sterile areas (Curiel and Lelieveld, 2014; Raynor, 2016). Numerous studies have shown that filtration materials generally perform well against bacteria, fungi, or viruses, with filtration efficiencies ranging from 80 % to 99.9 % (Majchrzycka, 2014; Zou and Yao, 2014; Jeong et al., 2019).

However, these microorganisms trapped in the filter can rapidly multiply under the proper humidity, temperature, and nutrient conditions (Kemp et al., 2001; Kelkar et al., 2005). The filters may thus act as a source of secondary microbial pollution (Maus et al., 2001). Antibacterial agents (e.g., quaternary ammonium phosphate, polyhexamethylene, and nano silver) added to the filter material can inhibit the growth of microorganisms on the filter, but they are not widely used because they may react with the filter materials (Cecchini et al., 2004; Lee et al., 2010). UV irradiation, while able to inactivate viruses, also harms the skin and eyes. Therefore, researchers have considered installing such devices in air purifiers. However, UV irradiation can only play a limited role owing to the limited space in air purifiers. The average residence time of air inside the purification system is only a few seconds, whereas virus aerosols require a longer period of irradiation exposure for effective inactivation. Therefore, a single round of UV irradiation may struggle to effectively inactivate viruses within air purifiers (Yang et al., 2020; Moreno et al., 2021).

In this study, aerosol filtration and UV-C irradiation were combined to effectively deal with virus aerosols. Although the two combined technologies have been applied in air purifier equipment prior to this study, the characteristics of filter material interception and UV-C inactivation of virus aerosols were not fully investigated. Especially, the virus's small size makes it harder to intercept by filtration than bacteria, while its health risks are of greater concern during the COVID-19 pandemic. With the right filtration material, the viruses and other microorganisms in aerosols can be captured, thereby providing sufficient time for inactivation via UV-C irradiation, while also inhibiting the reproduction and enrichment of microorganisms on the filter material. Therefore, in this study, f2 and MS2 phages were used as model viruses to investigate the effects of varying parameters of the combined technologies for the removal and inactivation of virus aerosols.

2 Methods and materials

The bacteriophages f2 and MS2 were used to simulate COVID-19 in this study, and the virus aerosol removal performance by the combination of filtration and UV-C irradiation was investigated. The effects of different filter materials and filtration rates on viral aerosol filtration efficiency, and the effects of UV-C irradiation intensity, exposure time, and initial virus concentration on the inactivation efficiency were discussed. The number of viruses was detected using the double agar plate method. The filtration removal rate and inactivation removal rate were calculated by detecting the virus aerosols and virus concentrations on the filter material before and after filtration, respectively. The filtration and inactivation efficiency of bacteriophage f2 and MS2 was calculated as follows (Eq. (1)):

$$Re = \log N_0 - \log N_t = \log(N_0/N_t), \quad (1)$$

where Re represents the removal efficiency of viruses by filtration or inactivation, N_0 is the original concentration of the virus before filtration or inactivation, and N_t is the residual virus concentration after filtration or inactivation.

2.1 Filter materials

The four polypropylene melt-blown nonwoven filtering materials used for the bioaerosol tests were provided by the manufacturer Shenzhen China Textile Filters Nonwoven Fabric Co., Ltd. (China). The materials are classed into four filter levels depending on the test standards of GB/T14295-2008 and GB/T6165-2008 (China). We renamed the four polypropylene melt-blown nonwoven filtering materials as PP-1, PP-2, PP-3, and PP-4 based on their filtering levels. These filter materials are widely used in indoor air purification systems, and their detailed information is listed in Table 1. All filters were cut into discs of 6 cm in diameter before use. The size and morphology of filtering materials were observed using scanning electron microscopy (SEM, Hitachi S-4800, Japan).

Table 1 Basic parameters of filter materials

Filter material	Filter levels	Efficiency (%)	Test aerosol	Test standard
PP-1	High (A)	99.9	NaCl	GB/T6165-2008
PP-2	Sub-high (YG)	99.5	NaCl	GB/T14295-2008
PP-3	Middle (Z)	65.0	NaCl	GB/T14295-2008
PP-4	Low (C)	40.0	NaCl	GB/T14295-2008

2.2 Virus preparation and assay

The icosahedral bacteriophage f2 and MS2 were selected for the bioaerosols filtration and filter coating experiments, as they are smaller than most microorganisms, with sizes of 20–26 nm, and could thus properly reflect the minimum performance required for filter materials to remove microbial aerosols. Moreover, both phages have the same nucleic acid type as that of SARS-COV-2 (single-stranded RNA) and are smaller than the 60–140 nm size range of SARS-COV-2 (Leung and Sun, 2020; Zhu et al., 2020).

The f2 and MS2 phages and their host *Escherichia coli* were purchased from the Institute of Health and Environmental Medicine, Academy of Military Medical Sciences, China, and the culture process of phage f2 and MS2 was as follows. Approximately 1 mL of f2 or MS2 phage was placed in the *Escherichia coli* culture medium and incubated in a shaker at 37 °C for 24 h. After centrifugation and purification at 4000 r/min for 10 min, the supernatant was filtered through a 0.22 μm polyvinylidene fluoride (PDVF) microporous material filter, and the phage filtrate was stored at 4 °C. The f2 and MS2 phages were cultured by the double agar plate method and counted as plaque forming units per mL (PFU/mL). Plaque quantities from 30 to 300 plates were considered to have been accurately counted (Cheng et al., 2014).

2.3 Filtration experiment

The experimental devices were composed of three main parts: virus aerosol production, filtration and detection. The first part was an organic glass chamber in which the virus aerosol was introduced by a nebulizer (TK-3, China). The ceiling fans in the organic glass chamber were specifically designed to homogenize the distribution of virus aerosol. The second part was a filter unit to which the test filter material was fixed by a plastic component. The homogeneous virus aerosol in the organic glass containers was carried into the plastic components through a rubber hose. The funnel-shaped internal space of the plastic components was specifically designed to ensure uniform face velocity at the tested filter material and a homogenous coating of aerosolized microorganisms on the filter material. Most virus aerosols are intercepted by the filter material, and a few virus aerosols pass through the filter material to the next collection stage. The third part was a virus aerosol collecting unit. The virus aerosols from the blank and experimental groups were collected by a liquid impact decay biological sampler (AGI-303, China) (Fig. 1). AGI-303 consists of a glass sampling bottle, bracket, and absorption solution, and is suitable for the sampling of microbial aerosols. Multiple microorganisms in the microbial particle group can be released and evenly distributed in the sampling liquid owing to the air flow and agitation of the sampling liquid during the sampling process. The number of microorganisms in the air can be accurately measured after further culturing. An adjustable flow meter was used to regulate and monitor the flow, thus indirectly controlling the wind speed through the tested filter material.

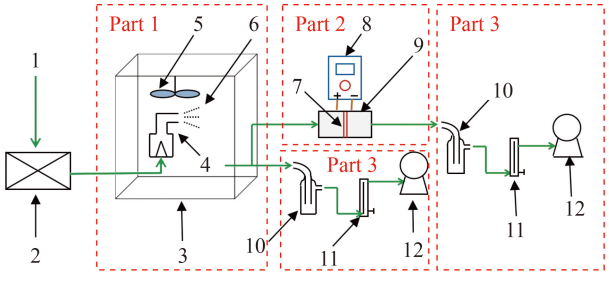

1-Air; 2-HEPA filter; 3-organic glass chamber; 4-TK-3 nebulizer; 5-ceiling fans; 6-virus aerosol; 7-filter material; 8-micro-manometer; 9-filter holder; 10-biological sampler (AGI-303); 11-flow meter; 12-pump.

Fig. 1 Schematic diagram of the experiment for trapping virus aerosol by the filtration material.

2.4 Inactivation experiment

The UV-C inactivation experimental device is shown in Fig. 2. First, the air carrying the virus aerosol was passed through the filter material for 1 h to intercept and enrich phage aerosols. The number of phages enriched on the filter material was varied by changing the concentration of the phage solution in the aerosol generator to obtain different concentrations of microbial aerosols. The virus-rich filter material was then cut into two sections, one piece as a control group that was placed in an opaque box without a UV-C lamp, and the other one as an experimental group placed in an opaque box equipped with a UV-C lamp. Then, a radiometer (UVC-254, Japan) was used to measure the irradiation intensity on the filter material in the experimental group, which was adjusted by changing the distance between the filter film and UV-C lamp. The filter materials of the control and experimental groups were taken out at the allocated time, eluted by PBS eluent, and detected by the double agar plate method. The inactivation rate was then calculated.

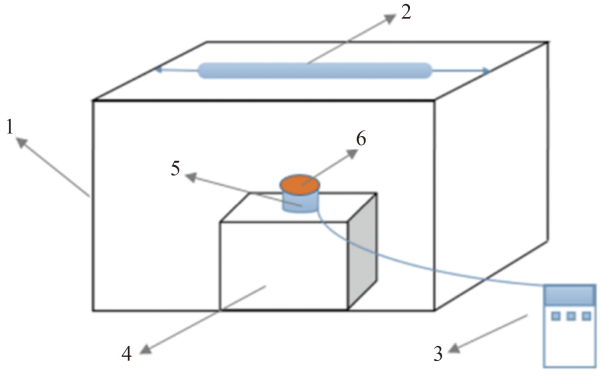

1-Light tight box; 2-UV-C lamp; 3-radiometer; 4-height adjustment platform; 5-illuminometer probe; 6-filter material with enriched virus.

Fig. 2 Schematic diagram of the experimental device for inactivating virus by UV-C irradiation.

2.5 Detection of virus coated on filters

The virus-rich filter samples—both irradiated and non-irradiated—were cut into several smaller fragments, which were then added to a glass test tube filled with 10 mL PBS eluent and shaken for 60 s to elute the viruses coated on the filter material (Pigeot-Remy et al., 2014). Then, the double agar plate method was used for culturing and counting the concentrations of the viruses.

3 Results and discussion

3.1 Scanning electron microscope (SEM) analysis

The SEM images of various filter materials are shown in Fig. 3. It can be seen that the fibers of several filter materials were smooth and evenly distributed. In the typical structure of melt-blown nonwoven fabrics, circular staggered fibers form a fiber web. It can also be seen from Fig. 3 that the diameter of the PP-1 fiber was relatively uniform, with a coarse fiber diameter of approximately 20 μm, and a fine fiber diameter of approximately 10 μm. In contrast, the diameter differences in PP-2 and PP-3 fibers were more obvious, indicating that the PP-1 material had higher filtration precision. The diameter range of the PP-2 fibers was 1–20 μm, and that of PP-3 fibers was 1–40 μm. The diameter of PP-4 fibers was the thickest, with that of the thickest fibers exceeding 100 μm.

The SEM micrographs of filter materials after virus filtration are shown in Fig. 4. It can be seen that a large number of virus aerosol droplets were attached to the fibers of the PP-1 filter materials, and that the size of most droplets was between 0.5 and 3 μm.

3.2 Wind resistance of filter material

Fig. 5 shows the change in wind resistance caused by the

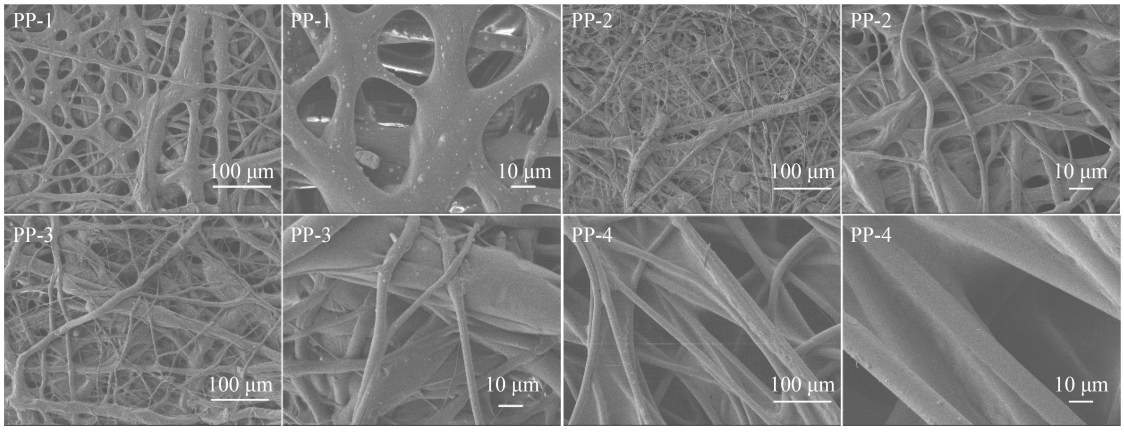

Fig. 3 SEM micrographs of filter materials (PP-1, PP-2, PP-3, PP-4).

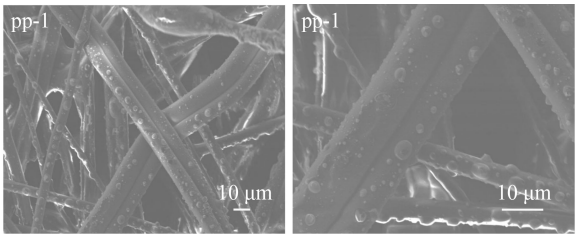

Fig. 4 SEM micrographs of PP-1 filter materials after virus filtration.

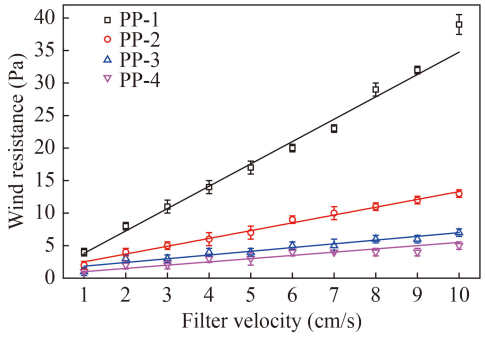

Fig. 5 Wind resistance of various materials with changing filter velocity.

four PP materials at different filtration speeds. The results showed that with the filtration speed range of 1–10 cm/s, the material wind resistance was proportional to the filtration speed, presenting a linear relationship. Detailed parameters are shown in Table 2. Among the four PP materials, PP-1 had the fastest pressure drop rate with an increase in filtration speed, while PP-4 had the lowest rate. This was related to the degree of precision of the materials, where the more precise materials experienced a greater pressure drop.

Table 2 Wind resistance performance of filter material

Filter material	R^2	Slope	Intercept
PP-1	0.981	3.65	−0.40
PP-2	0.992	1.21	1.27
PP-3	0.871	0.31	1.20
PP-4	0.936	0.57	1.27

The wind resistance of filter material was the key factor affecting the air volume that passed through. The lower the wind resistance, the higher the ventilation volume. In a previous study (Majchrzycka, 2014), the air flow resistance demonstrated by polylactic acid (PLA) and PLA modified with Bioperlite (PLA + Bioperlite) was 202–322 Pa. The maximum wind resistance of the filter materials selected in the present study was only 40 Pa, which is lower than the wind resistance of most high-efficiency filter materials.

3.3 Distribution of virus aerosol particle size

The filter material selected in this experiment was mainly used to remove microorganisms in the air through filtration and retention. As for the filtration technology, the particle size of microbial aerosols plays a decisive role in filtration performance. Therefore, the particle size and particle size distribution of microbial aerosols need to be determined before testing the performance of filter materials material. In this study, f2 and MS2 phage viruses, which are commonly used, were selected to simulate microorganism aerosols of the smallest sizes in the air, and the filtration performance of different filter materials was investigated. The initial concentration of 2.0×10^8 PFU/mL phage solution was prepared and added into TK-3 microbial aerosol generator. Of this, 0.3 mL phage solution was converted into microbial aerosol every minute for 10 min. The particle size distribution of microbial aerosols was measured by sampling with a six-stage Anderson sampler (JMT-6, China) for 1 min, as shown in Fig. 6.

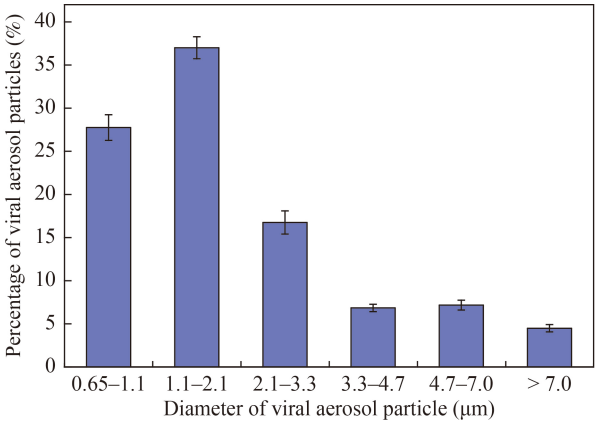

Fig. 6 Distribution of virus aerosol particle sizes.

The results showed that the minimum particle size of MS2 and f2 phage aerosols was less than 1 μm, and the maximum particle size was more than 7 μm. The range was mainly concentrated within 0.65–3.3 μm, with particle sizes of 0.65–1.1 μm accounting for 27.7 %, 1.1–2.1 μm for a maximum of 37 %, and 2.1–3.3 μm for only 14.7 % of all particles. Pigeot-Remy et al. (2014) measured the particle sizes of microbial aerosols, which were mainly distributed in the range of 0.65–1.0 μm. In our study, the particle size distribution range of virus aerosols was much wider and larger, which may be because of the use of different microbial aerosol generators or different measurement methods. Furthermore, the abundance of particles of other sizes was low, which differed from the distribution structure characteristics of the f2 and MS2 phages at 20–26 nm. This phenomenon may be because of the condensation of the phages into virus aerosols when they are encapsulated in small droplets during the atomization process, which is similar to the virus aerosols produced by the human body through sneezing (Kalogerakis et al., 2005).

3.4 Interception characteristics of the filter material

3.4.1 Effects of different filter materials on the interception performance of virus aerosols

The performance of different filtration materials on f2 and MS2 virus aerosols is shown in Fig. 7 (the filtration rate was 5.3 cm/s, and the initial concentration was 2.0×10^5 PFU/m^3). The results showed that the materials with high filtration precision demonstrated a higher interception rate for virus aerosols. The interception performance of PP-1 filter material for f2 microbial aerosols was more than 2 log, and the interception performance for MS2 microbial aerosols was up to 3 log. The performance of the PP-4 material presented the lowest interception rate of less than 1 log for two phages. This means that high-precision commercial filter materials can effectively remove all kinds of microorganisms from the air.

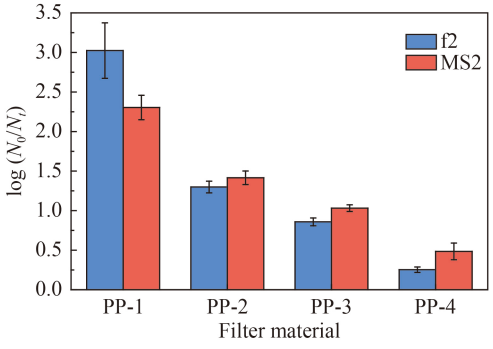

Fig. 7 Interception performance of f2 and MS2 aerosols by different filter materials.

A previous study (Majchrzycka, 2014) determined the filtration efficiency of polylactic acid (PLA) and PLA modified with Bioperlite (PLA +Bioperlite) for *S. aureus* and *P. aeruginosa* is to be 94.96 %–99.34 %. Another result showed that the filtration efficiency of most mask filter materials for particles with sizes of 0.37–20 μm was more than 90 %, and the filtration efficiency of N95 masks was more than 99 (Zou and Yao, 2014). This matches the efficiency of the PP-1 filter material for the virus aerosols used in our study indicating that the PP-1 filter material has adequate filtration efficiency to meet the protection requirements (Technical committee CEN/TC 79 "Respiratory protective devices", 2009).

3.4.2 Effects of filtration rates on the interception of virus aerosols

To guide the design of a reasonable filtration rate for microbial aerosol interception, the influence of filtration rate on microbial interception by filter materials should be investigated. Herein, the interception performance of the PP-1 filter material for f2 and MS2 phage aerosols that had initial concentrations of 2.0×10^5 PFU/m^3 was tested at the filtration rates of 1, 3, 5, and 7 cm/s, as shown in Fig. 8.

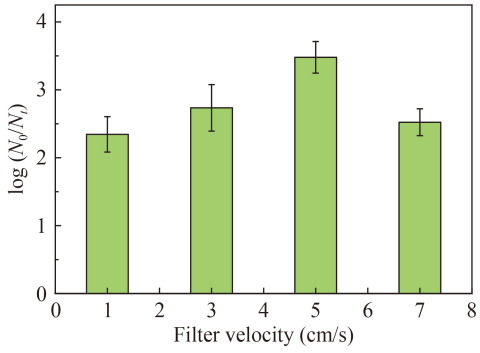

Fig. 8 Influence of filtration rate on the f2 aerosols trapped in the PP-1 filter material.

The filtration mechanism of HEPA filter includes interception, precipitation, impact, diffusion, and electrostatic adsorption, etc. (Curiel and Lelieveld, 2014). Within the filtration rate range of 1–7 cm/s, the interception performance of the filter material first increased and then decreased with an increase in filtration rate, and the PP-1 material led to the greatest interception of f2 phages at a filtration rate of 5 cm/s. The reason for this phenomenon is most likely because of the strengthened interception performance by an increase in inertial collision at higher filtration speeds, although in this situation, the interception performance via free diffusion becomes weaker. The best interception performance occurs when the two interception modes work together.

It is noteworthy that the interception contribution of inertial collision and free diffusion is affected by filter material performance and particle size distribution, and the optimal interception speed can be much greater or lower than 5 cm/s. However, according to the experimental results of this study, when high-precision filter materials such as PP-1 are used to intercept virus aerosols, the filtration rate should be as close to 5 cm/s as possible.

3.5 Effects of UV-C on virus aerosol inactivation

3.5.1 Effect of UV-C intensity on virus aerosol inactivation process

The microorganism concentrated on the filter material pose a serious threat to indoor air quality, so it is necessary to inactivate them on the filter material. In this experiment, a 254 nm UV-C lamp with good sterilization effect and reliable operating duration was selected to conduct the experiment, to investigate the influence of irradiation intensity and time on sterilization, and to

optimize the experimental parameters. Phage aerosols with initial concentrations from 2.0×10^7 to 2.0×10^8 PFU/m^3 were prepared and continuously passed through a material at a filtration rate of 5.3 cm/s for 1 h, so that the number of viruses concentrated on each material was from 5.0×10^6 to 5.0×10^7. The duration of UV-C exposure for the inactivation of f2 and MS2 phages was set to 30 min, which demonstrated an inactivation trend varying with UV-C irradiation intensity, as shown in Fig. 9.

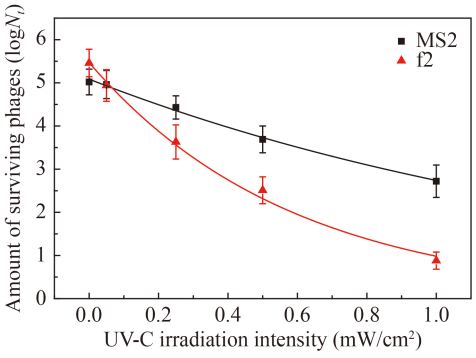

Fig. 9 Effect of the intensity of UV-C irradiation on the inactivation of f2 and MS2 phages.

SPSS 19.0 software was used to curve fit the pair values of f2 and MS2 viruses that survived the 30 min of irradiation with various irradiation intensities. It was found that the fitting was the best when using an exponential function. The exponential fitting results of f2 and MS2 viruses were as follows (Eqs. (2) and (3)):

$$\log(f2) = 5.5e^{-1.7x}, R^2 = 0.995, \quad (2)$$

$$\log(MS2) = 5.1e^{-0.62x}, R^2 = 0.994, \quad (3)$$

where x is the variable of irradiation intensity, and the unit is mW/cm^2. The log value of viable viruses decreased with an increase in UV-C irradiation intensity, but the rate of decline decreased, indicating that the improvement in the inactivation effect was limited with a further increase in irradiation intensity.

The survival of f2 and MS2 phages decreased with increasing irradiation intensity, and the slope of the survival number also decreased with increasing irradiation intensity. The inactivation effect of UV-C irradiation on f2 phages was better than that on MS2 phages. The difference in the resistance of different viruses to disinfection may result from the complexity of protein capsids and nucleic acids (Thurston-Enriquez et al., 2005; Tseng and Li., 2006). The protein capsid of the MS2 phage was likely more resistant to UV irradiation than that of the f2 phage, which allowed the MS2 phage to have a greater resistance to UV irradiation. Therefore, the residual f2 phage was lower than the MS2 phage concentration under the same conditions. Typically, bacteria have stronger resistance to UV-C irradiation than viruses (McDonnell and Burke, 2011). As demonstrated in our study, virus aerosols were inactivated faster than bacterial aerosols under UV-C irradiation, as more than 99 % of f2 and 90 % of MS2 phages retained by PP-1 filters were inactivated within 0.5 h at an irradiation dosage of 9.0×10^3 mJ/cm^2. However, in the literature, it has been demonstrated that 99 % of aerosol bacteria retained by AC filters (polyester fibres with an inner activated charcoal layer) could only be inactivated within 4 h at the dosage of 5.18×10^4 mJ/cm^2 (Pigeot-Remy et al., 2014).

3.5.2 Inactivation effects of UV-C on virus aerosols based on exposure time

In this experiment, a microbial aerosol with an initial concentration of 2.0×10^7–2.0×10^8 PFU/m^3 was prepared and continuously passed through a filter material at a filtration rate of 5.3 cm/s for 1 h, so that the number of microorganisms concentrated on each material was 5.0×10^6–5.0×10^7 PFU. Fig. 10 showed the trend of the inactivation ability of UVC-254 against f2 and MS2 phages with an increase in irradiation time at different irradiation intensities. Under the same UV-C irradiation time but increased radiation intensity, the survival of f2 phages decreased. This can be explained by not only the increased molecular damage of viral nucleic acid, but also the irradiation at a higher intensity to reach further inside the filter material, thus exposing more virus aerosols to effective UV-C irradiation.

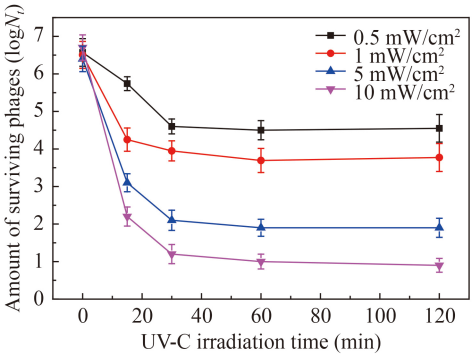

Fig. 10 Effects of the exposure time to UV-C lamp on f2 phages.

Although the number of viable f2 phages decreased with an increase in UV-C exposure duration from 0 to 30 min, under the same light intensity, there was no further increase in inactivation from exposure after 30 min. This is likely because while any f2 phages attached to the surface of the filter material were inactivated by UV-C irradiation within 30 min, the virus aerosol particulates that had entered the inner filter material and could not be exposed to UV-C irradiation, thus allowing their survival for much longer durations. Prior studies

have shown that the amount of bacteria coated on an AC filter does not decrease after 6 h of UV-A irradiation or after 4 h of UV-C irradiation, indicating a similar effect where the bacteria in shallow layers are sufficiently inactivated within a few hours, but those in the inner activated charcoal layer of the AC filter cannot be exposed to a sufficient UV-C dose to be permanently damaged.

However, bacteria retained by glass fiber filters could be completely inactivated, which can be explained by glass fiber's better light transmittance and thinness. At 0.42 mm thick, glass fiber filters are only 1st/6th the thickness of an AC filter, thus sufficiently exposing all bacteria to UV-C radiation (Pigeot-Remy et al., 2014). In this study, the PP-1 filter comprised a polypropylene electret melt-blown nonwoven material with a thickness of 0.5 mm. The experimental results showed that, just as for the AC filter material in the aforementioned literature, there was a limit to inactivation under UV-C irradiation. This may be because the internal structure and light transmittance of the PP-1 filter material are different from those of glass fiber filters.

Recently, another study showed that more than 5-log (99.999 %) of *E. coli* coated on a glass slide could be inactivated directly exposed to UV-C irradiation at a dosage of 30 mJ/cm^2 (Schnell et al., 2021). In our study, however, less than 50 % of f2 phages were inactivated by UV-C irradiation at a dosage of 90 mJ/cm^2. This further confirms that the filter material has a shielding effect on the virus. The fiber network structure of the filter material shielded the virus aerosols from UV-C irradiation, causing the UV-C intensity received by f2 aerosols distributed in the filter material to be lower than that reaching the surface of the filter material. Therefore, to avoid high virus enrichment in the internal filter material, we need to use UV-C irradiation to inactivate the virus intercepted on the surface of the filter material, and choose materials with good light transmittance, such as glass fiber. Despite these improvements, it is still inevitable that some viruses will enter the filter material, but these could be inactivated by adding UV-C irradiation on the other side of the filter. To inactivate microorganisms in the filter material, the irradiation time and intensity should be appropriately increased to ensure a sufficient dosage of irradiation for effectively inactivating microbial aerosols.

3.5.3 Effects of the initial phage concentration on inactivation process

The effect of the initial virus concentration on the removal effect is shown in Fig. 11. The results showed that as the concentration of f2 phages on the filter gradually increased, the inactivation efficiency by UV-C irradiation decreased (the total number of inactivated f2 phages increased). This may be because, at a higher initial concentration, phages on the outer surface had a shielding effect on the inside phages, resulting in a lower proportion of inactivated viruses. This indicated that the UV-C irradiation frequency needs to be increased to prevent the surface of the filter materials from being clogged by an excessive enrichment of viruses.

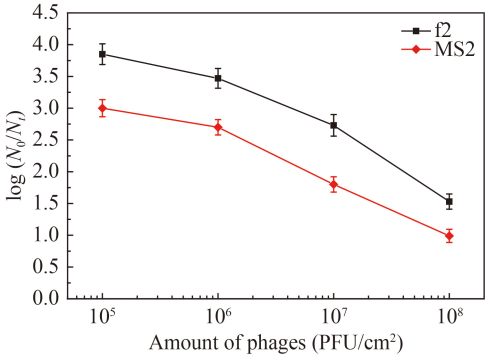

Fig. 11 Effects of the initial phage concentration on inactivation efficiency.

4 Conclusions

The combined filtration and UV-C irradiation proposed in this study can dynamically, continuously, and efficiently remove microbial aerosols. And there is an optimal ventilation speed for virus aerosol filtration. The log value of the surviving viruses trapped by the filter material decreased exponentially with an increase in UV-C irradiation intensity, which indicated that an excessive increase in irradiation intensity has little effect on improving the inactivation efficiency. Similarly, UV-C has an inactivation threshold for virus aerosols trapped by the filter material, which can not be inactivated even by increasing the irradiation. Moreover, the higher the initial concentration of viruses trapped by the filter, the lower the inactivation efficiency, mainly because of the blocking effect of virus aerosols. The air that is moved through indoor air ventilation systems can be effectively, efficiently, and economically purified via a filter design that uses a light-transmissible material, provides an adequate ventilation speed, and exposes the virus aerosols to UV radiation at a proper dosage for a sufficient duration. Such air filtration is essential for the development and application of indoor air pollution control technology.

Acknowledgements The research was supported by the National Natural Science Foundation of China (No. 52070192), which was greatly acknowledged.

References

Bazant M Z, Bush J W M (2021). A guideline to limit indoor airborne transmission of COVID-19. PNAS, 118(17): 1–12

Berry G, Parsons A, Morgan M, Rickert J, Cho H (2022). A review of methods to reduce the probability of the airborne spread of COVID-

19 in ventilation systems and enclosed spaces. Environmental Research, 203: 111765

Castrillón S R V, De Lasa H I (2007). Performance evaluation of photocatalytic reactors for air purification using computational fluid dynamics (CFD). Industrial & Engineering Chemistry Research, 46(18): 5867–5880

Cecchini C, Verdenelli M C, Orpianesi C, Dadea G M, Cresci A (2004). Effects of antimicrobial treatment on fiberglass-acrylic filters. Journal of Applied Microbiology, 97(2): 371–377

Chen Q (2021). Can we migrate covid-19 spreading risk. Frontiers of Environmental Science & Engineering, 15(3): 35

Cheng R, Li G, Cheng C, Liu P, Shi L, Ma Z, Zheng X (2014). Removal of bacteriophage f2 in water by nanoscale zero-valent iron and parameters optimization using response surface methodology. Chemical Engineering Journal, 252: 150–158

Correia G, Rodrigues L, Gameiro da Silva M, Gonçalves T (2020). Airborne route and bad use of ventilation systems as non-negligible factors in SARS-CoV-2 transmission. Medical Hypotheses, 141: 109781

Curiel G J, Lelieveld H (2014). Process hygiene | risk and control of airborne contamination. In: Batt C, Patel P, eds. Encyclopedia of Food Microbiology (2nd Edition). New York: Academic Press, 200–206

Dancer S J, Tang J W, Marr L C, Miller S, Morawska L, Jimenez J L (2020). Putting a balance on the aerosolization debate around SARS-CoV-2. Journal of Hospital Infection, 105(3): 569–570

Jeong S B, Ko H S, Seo S C, Jung J H (2019). Evaluation of filtration characteristics and microbial recovery rates of commercial filtering facepiece respirators against airborne bacterial particles. Science of the Total Environment, 682(10): 729–736

Jiang G, Wang C, Song L, Wang X, Zhou Y, Fei C, Liu H (2021). Aerosol transmission, an indispensable route of covid-19 spread: case study of a department-store cluster. Frontiers of Environmental Science and Engineering, 15(3): 46

Kalogerakis N, Paschali D, Lekaditis V, Pantidou A, Eleftheriadis K, Lazaridis M (2005). Indoor air quality—bioaerosol measurements in domestic and office premises. Journal of Aerosol Science, 36(5–6): 751–761

Kelkar U, Bal A M, Kulkarni S (2005). Fungal contamination of air conditioning units in operating theatres in India. Journal of Hospital Infection, 60(1): 81–84

Kemp P C, Neumeister-Kemp H G, Lysek G, Murray F (2001). Survival and growth of micro-organisms on air filtration media during initial loading. Atmospheric Environment, 35(28): 4739–4749

Klepeis N E, Nelson W C, Ott W R, Robinson J P, Tsang A M, Switzer P, Behar J V, Hern S C, Engelmann W H (2001). The national human activity pattern survey (NHAPS): a resource for assessing exposure to environmental pollutants. Journal of Exposure Analysis and Environmental Epidemiology, 11(3): 231–252

Lee B U, Yun S H, Jung J H, Bae G N (2010). Effect of relative humidity and variation of particle number size distribution on the inactivation effectiveness of airborne silver nanoparticles against bacteria bioaerosols deposited on a filter. Journal of Aerosol Science, 41(5): 447–456

Leung W W F, Sun Q (2020). Electrostatic charged nanofiber filter for filtering airborne novel coronavirus (COVID-19) and nano-aerosols. Separation and Purification Technology, 250: 116886

Majchrzycka K (2014). Evaluation of a new bioactive nonwoven fabric for respiratory protection. Fibres & Textiles in Eastern Europe, 22(1): 81–88

Maus R, Goppelsröder A, Umhauer H (2001). Survival of bacterial and mold spores in air filter media. Atmospheric Environment, 35(1): 105–113

McDonnell G, Burke P (2011). Disinfection: Is it time to reconsider Spaulding. Journal of Hospital Infection, 78(3): 163–170

Moreno E, Klochok G, García S (2021). Active versus passive flow control in UVC filters for COVID-19 containment. Annals of Biomedical Engineering, 49(9): 2554–2565

Peters A, Parneix P, Otter J, Pittet D (2020). Putting some context to the aerosolization debate around SARS-CoV-2. Journal of Hospital Infection, 105(2): 381–382

Pigeot-Remy S, Lazzaroni J C, Simonet F, Petinga P, Vallet C, Petit P, Vialle P J, Guillard C (2014). Survival of bioaerosols in HVAC system photocatalytic filters. Applied Catalysis B: Environmental, 144: 654–664

Raynor P C (2016). Chapter 7—Controlling nanoparticle exposures. In: Ramachandran G, ed. Assessing Nanoparticle Risks to Human Health (2nd Edition). Norwich, NY: William Andrew, 167–193

Santos A F, Gaspar P D, Hamandosh A, Aguiar E B, Guerra Filho A C, Souza H J L (2020). Best practices on HVAC design to minimize the risk of COVID-19 infection within indoor environments. Brazilian Archives of Biology and Technology, 63: e20200335

Schnell E, Karamooz E, Harriff M J, Yates J E, Pfeiffer C D, Smith S M (2021). Construction and validation of an ultraviolet germicidal irradiation system using locally available components. PLoS One, 16(7): e0255123

Technical committee CEN/TC 79 “Respiratory protective devices”, (2009). European standard EN 149:2001+A1: Respiratory protective devices – Filtering half masks to protect against particles – Requirements, testing, marking. London: British Standards Institution.

Thurston-Enriquez J A, Haas C N, Jacangelo J, Gerba C P (2005). Inactivation of enteric adenovirus and feline calicivirus by ozone. Water Research, 39(15): 3650–3656

Tseng C C, Li C S (2006). Ozone for inactivation of aerosolized bacteriophages. Aerosol Science and Technology, 40(9): 683–689

Xie W, Li Y, Bai W, Hou J, Ma T, Zeng X, Zhang L, An T (2021). The source and transport of bioaerosols in the air: a review. Frontiers of Environmental Science and Engineering, 15(3): 44

Yang H, Hu J, Li P, Zhang C (2020). Ultraviolet germicidal irradiation for filtering facepiece respirators disinfection to facilitate reuse during COVID-19 pandemic: a review. Photodiagnosis and Photodynamic Therapy, 31: 101943

Zhu N, Zhang D, Wang W, Li X, Yang B, Song J, Zhao X, Huang B, Shi W, Lu R, et al., the China Novel Coronavirus Investigating and Research Team (2020). A novel coronavirus from patients with pneumonia in china, 2019. New England Journal of Medicine, 382(8): 727–733

Zou Z, Yao M (2014). Airflow resistance and bio-filtering performance of carbon nanotube filters and current facepiece respirators. Journal of Aerosol Science, 79(2015): 61–71